



RESEARCH PAPER



Upregulated circRNA hsa_circ_0071036 promotes tumourigenesis of pancreatic cancer by sponging miR-489 and predicts unfavorable characteristics and prognosis

Xu Han ^{a,*}, Yuan Fang^{a,*}, Pingping Chen^{b,*}, Yaolin Xu ^a, Wentao Zhou^a, Yefei Rong^a, Jian-Ang Li^a, Wei Chen^c, and Wenhui Lou^a

^aDepartment of General Surgery, Zhongshan Hospital, Fudan University, Shanghai, China; ^bDepartment of Assisted Reproduction, Xinhua Hospital, Shanghai Jiaotong University School of Medicine & Molecular Genetics Group, Shanghai Institute for Pediatric Research, Shanghai, China; ^cDepartment of Anesthesia, Zhongshan Hospital, Fudan University, Shanghai, China

ABSTRACT

Circular RNAs (circRNAs), the new stars of endogenous non-coding RNAs, are dysregulated in various tumors including pancreatic cancer. Here, we aimed to investigate the biological functions of hsa_circ_0071036 in the tumourigenesis and progression of pancreatic ductal adenocarcinoma (PDAC) and its clinical implications. The differential expression profile of circRNAs in 4 pairs of PDAC tissues was analyzed by microarray assay. Quantitative real-time PCR and fluorescence in situ hybridization (FISH) were utilized to determine the expression patterns and their clinical significance. Functional experiments *in vitro* and *in vivo* were performed to explore whether hsa_circ_0071036 functions as an oncogenic circRNA in PDAC. Mechanistically, RT-qPCR, dual luciferase reporter and RNA pull-down assays were conducted to identify the interaction between hsa_circ_0071036 and miR-489 in PDAC. Hsa_circ_0071036 was remarkably overexpressed in PDAC cell lines and tissue samples, which negatively correlated with miR-489 expression. Aberrant expression of hsa_circ_0071036 correlated with poor clinicopathological characteristics and prognoses of PDAC patients. Knockdown of hsa_circ_0071036 suppressed proliferation and invasion and induced apoptosis *in vitro*. Moreover, the *in vivo* xenograft model confirmed that silencing of hsa_circ_0071036 attenuated tumor growth. Mechanistic analyses indicated that hsa_circ_0071036 acted as an efficient miRNA sponge for miR-489 in PDAC. In summary, our study revealed that upregulated hsa_circ_0071036 promotes PDAC pathogenesis and progression by directly sponging miR-489, which implies an important role for this circRNA-miRNA functional network.

ARTICLE HISTORY

Received 15 November 2019
Revised 19 September 2020
Accepted 5 January 2021

KEYWORDS

Circrnas; pancreatic cancer; hsa_circ_0071036; miR-489; tumourigenesis

Introduction


Pancreatic ductal adenocarcinoma (PDAC), generally regarded as pancreatic cancer, is a highly aggressive and one of the most lethal malignancies with a 5-year overall survival rate of less than 8% [1,2]. Unfortunately, there has been no apparent improvement in the life expectancy of PDAC patients over the last few decades [3,4]. PDAC lacks effective and reliable treatments mainly due to the inadequacy of both molecular characteristics and potential therapeutic targets. Hence, there is a pressing need to explore novel molecular mechanisms underlying the tumourigenicity of pancreatic cancer.

Circular RNAs (circRNAs), which comprise a novel class of widespread non-coding RNAs that

broadly regulate gene expression, are produced by back-splicing of precursor mRNA and are widely expressed in eukaryotic cells [5–7]. Many circRNAs are known to be oncogenes or tumor suppressors, further complicating the biology of human malignant tumors [8]. Some studies have implied that aberrant expression of circRNAs may serve as diagnostic or prognostic biomarkers or potential therapeutic targets for numerous cancers [9,10]. Specifically, recent results have revealed a link between altered circRNAs and pathogenesis in PDAC [11]. One important molecular mechanism of circRNAs involved in tumourigenesis is that circRNAs act as competing endogenous RNA (ceRNA) to repress the expression of their targeted miRNAs, thereby regula

CONTACT Wenhui Lou  lou.wenhui@zs-hospital.sh.cn, louzsh@126.com  Wei Chen  chen.wei@zs-hospital.sh.cn; Xu Han han.xu1@zs-hospital.sh.cn

*Xu Han, Yuan Fang and Pingping Chen contributed equally to this work.

 Supplemental data for this article can be accessed [here](#).

© 2021 Informa UK Limited, trading as Taylor & Francis Group

ting the specific genes targeted by miRNAs [8–11]. However, the mechanisms underlying the dysregulation of circRNAs in tumorigenesis and the involvement of regulatory downstream miRNAs remain largely unknown in pancreatic cancer.

Preliminarily, we screened a series of circRNA candidates that are differentially expressed in PDAC tissues compared with matched normal tissues by circRNA microarray. We identified one key circRNA derived from the *INPP4B* gene and termed it hsa_circ_0071036 (alias: hsa_circ_1003

95). Our previous studies revealed a regulatory axis centered on miR-489 as a tumor suppressor that plays an important role in oncogenic *KRAS*-driven PDAC metastasis. Oncogenic *KRAS* activates *NF- κ B-YY1*, thus attenuating the level of miR-489 and thereby promoting tumor progression and metastasis [12]. Interestingly, we mined public databases and the results suggested that miR-489 possessed a binding site for hsa_circ_0071036. Therefore, we speculated that hsa_circ_0071036 could sponge miR-489 to modulate its downstream function. This study aimed to determine the circRNA hsa_circ_0071036 expression pattern in PDAC and its clinical implications, indicating its potential as a diagnostic marker, prognostic predictor and therapeutic target. Functional experiments *in vitro* and *in vivo* were then performed to explore the potential molecular actions of hsa_circ_0071036 in mediating PDAC tumorigenesis and progression. Furthermore, we also focused our attention on the interaction between hsa_circ_0071036 and miR-489 that affects the pathogenesis of PDAC in the present study.

Materials and methods

Patients and pancreatic cancer specimens

Pancreatic ductal adenocarcinoma tissues (cohort 1, n = 56; cohort 2, n = 90) and corresponding adjacent normal pancreas tissues were obtained from patients who underwent radical surgery with regional lymph node resection at the Department of Pancreatic Surgery, Zhongshan Hospital, Fudan University between 2016 and 2018. None of these patients had received preoperative chemotherapy or radiotherapy. Institutional Review Board approval and patient informed consent were obtained for this study.

Clinical data were obtained and analyzed retrospectively from the Pancreatic Tumor Registry. The detailed clinicopathologic characteristics are summarized in Table 1. Follow-up information was collected from the Pancreatic Tumor Registry at Zhongshan Hospital, Fudan University. The duration of overall survival (OS) was calculated from the date of operation until tumor-specific death or the patient's last follow-up.

CircRNA microarray

We conducted human circRNA array analysis of 4 paired PDAC samples based on the Arraystar standard protocols (Kangchen Bio-tech, Shanghai). Total RNA was quantified using the NanoDrop ND-1000. Additionally, RNA integrity was verified by electrophoresis on a denaturing agarose gel. CircRNAs were then digested with RNase R (Epicenter, USA) to remove linear RNAs. The enriched circRNAs were amplified and labeled utilizing a random primer-based labeling system (Arraystar Super RNA Labeling Kit). Subsequently, array hybridization was performed (V2, 8x15K, Arraystar). Slides were scanned immediately after washing with the Agilent Scanner G2505 C. Quantile normalization and subsequent bioinformatic analysis were performed. Statistically significant differentially expressed circRNAs were illustrated by volcano plot filtering, fold change filtering and hierarchical clustering.

RNA extraction and real-time PCR

We investigated circRNA expression profiles using paired primary PDAC and corresponding adjacent normal pancreas tissues. Total RNA from cells or tissues was extracted using TRIzol reagent (Invitrogen). Quantified RNAs were reverse transcribed into cDNAs utilizing the Prime Script RT Master Mix. The qRT-PCR analyses were performed using the SYBR Select Master Mix Reagent (Applied Biosystems) according to the manufacturer's protocols. All reactions were run in triplicate to reduce bias. PCR primers for circRNAs were designed in divergent orientation. Relative expression values were normalized to GAPDH or U6 values and calculated using the $2^{-\Delta\Delta CT}$ method. The primers were as follows: *hsa_circ_00*

Table 1. Correlations between expression levels of hsa_circ_0071036 measured by qRT-PCR and clinicopathological characteristics at baseline (cohort 1).

Characteristics	High expression of hsa_circ_0071036 (n = 28)	Low expression of hsa_circ_0071036 (n = 28)	P value
Age at onset, mean (SD), y [†]	66.4 (9.2)	65.8 (9.8)	0.800
Male, n (%)	12 (42.9%)	17 (60.7%)	0.181
Female, n (%)	16 (57.1%)	11 (39.3%)	0.942
Tumor size, mean (median), cm [†]	3.6 (1.4)	3.5 (1.2)	
CA 19-9 level, mean (SD) U/mL [†]	373.7 (798.8)	364.4 (497.2)	0.959
CEA level, mean (SD) ng/mL [†]	4.8 (4.5)	9.0 (14.5)	0.156
Regional lymph node metastases, n (%)	25 (89.3%)	17 (60.7%)	0.014
PET-CT SUVmax, mean (SD) [†]	8.6 (3.0)	5.9 (2.0)	0.001
Location, n (%)			0.420
Head	14 (50.0%)	11 (39.3%)	
Distal	14 (50.0%)	17 (60.7%)	
Extrapancreatic organ invasion, n (%)	15 (53.6%)	11 (39.3%)	0.422
Neural invasion, n (%)	28 (100%)	27 (96.4%)	1.00
Vascular invasion, n (%)	7 (25.0%)	5 (17.9%)	0.515
Tumor microthrombus, n (%)	13 (46.4%)	9 (32.1%)	0.274
Necrosis, n (%)	4 (14.3%)	5 (17.9%)	1.00
Differentiation, n (%)			0.577
Grade 2	9 (32.1%)	11 (39.3%)	
Grade 2-3	19 (67.9%)	17 (60.7%)	
Ki-67 index, mean (SD) (%) [†]	41.1 (21.8)	38.6 (19.5)	0.653

NA = not applicable [†]continuous variable

71036 (*hsa_circRNA_103745*), F: GAGCCACGAGA TCCTTGCAT, R: TCCAGCACCGAAATTGTGG A; *miR-489*, F: ACACTCCAGCTGGGGTGACAT CACATATAC, R: CTCAACTGGTGTCTGGAG TCGG; *U6 RNA*, F: ACACTCCAGCTGGGCGCA AATTCGTGAAGC, R: CTCAACTGGTGTCTGG GAGTCGG; and *GAPDH*, F: TGACTTCAACAG CGACACCCA, R: CACCCTGTTGCTGTAGCCA AA. We defined those patients who ranked at the top 50% for expression level of hsa_circ_0071036 as the high expression group, while the rest were the low expression group.

Cell culture

The pancreatic cancer cell lines PANC-1, AsPC-1, H6C7, BxPC-3, MIA PaCa-2 were purchased from The Cell Bank of Type Culture Collection of the Chinese Academy of Sciences (CAS, Shanghai) and cultured in RPMI-1640 or DMEM supplemented with 10% fetal bovine serum (FBS) (Gibco, USA), 100 U/ml penicillin, and 100 µg/ml streptomycin. Cells were placed in an incubator at 37°C with 5%

CO₂. Cells in the logarithmic growth phase (80–90% confluent) were used for the experiments.

Cell invasion assay

The invasion potential of PANC-1 cells was assessed *in vitro* with a Matrigel invasion chamber (BD Biosciences, San Diego, USA). Briefly, cells (1 × 10⁵) in FBS-free medium were seeded into the upper chamber, and culture medium with 20% FBS was added into the lower chamber as a chemoattractant. Following incubation for 24 h, the invading cells that had penetrated through the Matrigel to the basal side of the membrane were fixed, stained, visualized and imaged. Random five high-power fields were observed for counting cell numbers.

Cell apoptosis analysis

For cell apoptosis, suspension tumor cells were analyzed by flow cytometry. Apoptotic cells were measured by Annexin V-APC staining (eBioscience, USA), and necrotic cells were detected by the

7-AAD exclusion method. Then, tumor cells were analyzed with a FACScan flow cytometer (BD Biosciences) according to the manufacturer's instructions.

Colony formation assay and cell proliferation assays

PANC-1 cells transfected with NC or si-hsa_circ_0071036 were seeded at a density of 800 cells per well into a 6-well plate and incubated for 11 days. The cells were washed with 1× phosphate-buffered saline (PBS), fixed for 30 min in 4% paraformaldehyde and stained for 15 min with crystal violet in methanol. The number of colonies was counted under a microscope.

Proliferation of transfected PANC-1 cells was evaluated by the Cell Counting Kit-8 (CCK-8) according to the manufacturer's protocol (Dojindo, Japan). After incubation, absorbance was determined at 450 nm at different times. Each experiment was performed in triplicate.

Gene expression vector construction and siRNA transfection

Small interfering RNAs (siRNAs) and overexpressed RNAs specific for hsa_circ_0071036, miR-489 mimic and negative control were synthesized by GeneChem (Shanghai, China). The 3' UTR segments of human hsa_circ_0071036 predicted to interact with miR-489 were amplified and cloned into a GV272 dual-luciferase vector. A lentiviral vector was utilized to silence hsa_circ_0071036 expression in cells. The vectors containing si-hsa_circ_0071036 and the negative control were designated LVpFU-GW-007 and LVpFU-GW-NC, respectively. All lentiviral infections (miRNA mimics and siRNAs) and selection of stable expression clones were performed according to the manufacturer's instructions (GeneChem, Shanghai, China).

Luciferase reporter system

PANC-1 cells were co-transfected with miR-489 mimics, firefly luciferase reporter GV272 vector containing the wild-type or mutant 3'UTR of hsa

_circ_0071036, and the control vector containing Renilla luciferase (GeneChem, Shanghai, China). Transfections were performed in triplicate and repeated in three independent experiments. After 48 h of transfection, luciferase activity was analyzed using a Dual-Luciferase Reporter Assay System (Promega, USA) according to the protocol. Firefly luciferase values were normalized to Renilla values to control for transfection efficiency.

RNA pull-down

Biotin-labeled hsa_circ_0071036 probe and negative control probe were synthesized (RiboBio, China). PANC-1 cells were lysed and incubated with specific hsa_circ_0071036 and control probes. Biotin-coupled RNA complexes were then pulled down by incubating the cell lysates with streptavidin-coated magnetic beads. The abundance of hsa_circ_0071036 and miR-489 was measured by qRT-PCR.

Tissue microarray (TMA) and fluorescence in situ hybridization (FISH)

To ensure uniform staining conditions of the tumors among all samples, TMA was performed for 90 samples (cohort 2). Each tumor was sampled in 2 regions, namely, pancreatic cancer and corresponding adjacent normal pancreas. Sections (4 μm) were cut from formalin-fixed paraffin-embedded tissues and placed onto silanized slides. Senior pathologists confirmed the histological diagnosis of PDAC for the TMA samples.

For circRNA FISH, cultured PANC-1 cells were fixed with 4% paraformaldehyde and then washed with 1× PBS, and paraffin-embedded sections (4 μm) from pancreatic cancer TMA were deparaffinized and rehydrated. The procedures were conducted with a specific Cy3-hsa_circ_0071036 FISH probe (Sangon Biotech, Shanghai) utilizing a RiboTM Fluorescent In Situ Hybridization Kit (RiboBio, China) according to the manufacturer's protocols. Hybridization was performed using a fluorescently labeled probe by incubation overnight, and then DAPI was stained. Images were captured and quantified by confocal microscopy

(DM6000 CFS, Leica). Cases were labeled hsa_circ_0071036 positive only if more than 10% of tumor cells were positive.

***In vivo* tumor xenograft model**

Four-week-old female BALB/c (nu/nu) mice were obtained and maintained in a specific pathogen-free (SPF) environment under constant conditions in the laboratory animal center of Zhongshan Hospital, Fudan University. Procedures involving animals and their care were conducted in accordance with the protocol approved by the Zhongshan Hospital Experimental Animal Ethics Committee (No. Y2017-012). For the xenograft tumor assay, transfected AsPC-1 cells with hsa_circ_0071036 knockdown (hsa_circ_0071036-KD) or negative control vector (5×10^6 cells/ml) were resuspended in 200 μ l of PBS and inoculated into the middle of the right armpit of nude mice (n = 6 per group). A week after inoculation, tumor growth was assessed by monitoring tumor volume ($TV = \pi/6 \times \text{length} \times \text{width} \times \text{width}$) twice per week. Finally, the nude mice were sacrificed, and the tumor foci were collected.

Statistical analysis and follow-up

The statistical analyses were performed using SPSS (Chicago, IL, version 16.0). Pearson's chi-square test, Fisher's exact test was used to compare proportions when appropriate, whereas means were compared using paired or unpaired Student's t test or non-parametric Mann-Whitney test. Pearson correlation and nonlinear exponential regression analysis were also performed. Survival analyses using the Kaplan-Meier curve were compared by log-rank test. A Cox proportional hazards model was performed to identify the factors independently associated with prognosis. Risk factors are described as hazard ratio (HR, 95% CI). Two-sided P values indicate the level of statistical significance (*, $P < 0.05$; **, $P < 0.01$; ***, $P < 0.001$). The duration of overall survival (OS) was calculated from the date of operation until tumor-specific death or the patient's last follow-up. The median follow-up time of cohort 2 was 20.8 months (range 44.3).

Results

Differential expression of circRNA hsa_circ_0071036 in PDAC

To identify key circRNAs involved in PDAC oncogenesis, we analyzed circRNA microarray data from 4 paired PDAC tissues and normal pancreas tissues. We detected 11,471 distinct circRNAs and a number of them were notably downregulated or upregulated in all four PDAC tissues, 84.9% of which consisted of protein-coding exons (Figure 1c). We identified 193 differentially expressed circRNAs based on fold change > 1.5 and p -value < 0.05 (Figure 1a,B), 120 of which were upregulated and 73 were downregulated. Among them, hsa_circ_0071036 was one of the most upregulated circRNAs in PDAC tissues (Figure 1d), which suggested that abnormal hsa_circ_0071036 expression may be related to PDAC oncogenesis.

Hsa_circ_0071036 was overexpressed in PDAC tissue samples and cell lines

To confirm the expression pattern of hsa_circ_0071036, qRT-PCR was further performed to investigate the expression levels of hsa_circ_0071036 in 56 pairs of PDAC tissues and corresponding adjacent normal pancreas tissues (cohort 1). The results indicated that hsa_circ_0071036 was significantly upregulated in PDAC tissues compared with the adjacent non-cancerous tissues (Figure 2a,B). Moreover, an ROC curve was generated to evaluate the potential of hsa_circ_0071036 as a diagnostic biomarker. Our data revealed that hsa_circ_0071036 could provide a good compromise between specificity and sensitivity, as shown by the ROC curve in Figure 2c, and the area under the ROC curve (AUC) was 0.65 ($P = 0.006$, 95% CI: 0.54–0.76).

Moreover, RNA-FISH was utilized to determine the localization and expression of hsa_circ_0071036 in PANC-1 cells and 90 paired PDAC tissue samples (cohort 2). Co-immunostained PANC-1 cells for circ_0071036 and DAPI showed that hsa_circ_0071036 was strongly and diffusely positive in both cytoplasmic and nuclear patterns (Figure 3a). Furthermore, hsa_circ_0071036 was

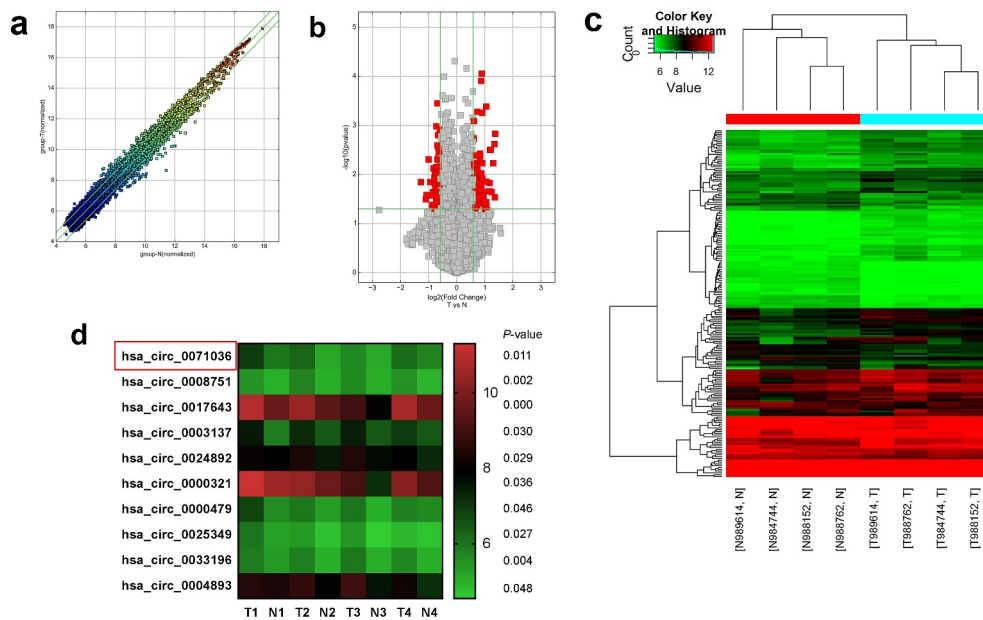


Figure 1. Expression profiles of circRNAs in PDAC. (a) The scatter plot visualizes the circRNA expression variation between PDAC and adjacent normal pancreas tissues. The space between two bar lines indicated more than a 1.5-fold change. (b) The volcano plot visualizes the expression of circRNA between PDAC and adjacent normal pancreas tissues. The red dots represent the differentially expressed circRNAs with statistical significance. (c) The hierarchical clustering of differentially expressed circRNAs and the dendrogram show the relationships among the expression levels in the samples. (d) The heat maps displayed the 10 most increased circRNAs.

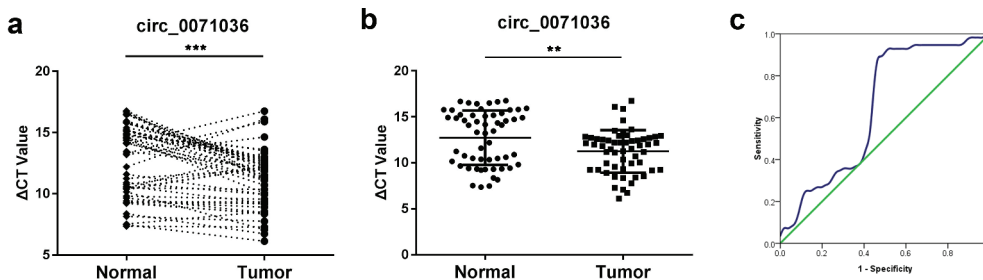


Figure 2. Overexpression of circ_0071036 (alias: hsa_circ_100395) in PDAC compared to adjacent normal pancreas tissues. (a) Relative expression of circ_0071036 in 56 cases of fresh human PDAC tissues and matched adjacent normal tissues by qRT-PCR (paired-samples t test), and those ranked at the top 50% expression level were considered to have high expression. (b) The circ_0071036 expression was remarkably upregulated in PDAC tissues compared to adjacent normal tissues (Student's t test). (c) To determine the diagnostic value of circ_0071036 in PDAC, an ROC graph was obtained with normal controls and PDACs, and the area under the curve was 0.65 ($P = 0.006$, 95% CI: 0.54–0.76).

positive in PDAC tissues when predominantly cytoplasmic staining was observed, and only a small number of cells were negative, whereas almost all normal ductal epithelial cells were negative for hsa_circ_0071036 in the adjacent normal tissues of the pancreas (Figure 3b). The percentages of PDAC tissues negative and positive for hsa_circ_0071036 expression in were 27.8% (25/90) and 72.2% (65/90), respectively. In contrast, miR-489 was negative in $KRAS^{G12D}$ mutant PDAC and

strongly positive in adjacent normal tissues of the pancreas (Figure S1).

Correlation of hsa_circ_0071036 expression with clinicopathological characteristics and prognosis

We next examined the associations between hsa_circ_0071036 expression and the clinicopathological parameters and prognosis of PDAC patients. First, we categorized hsa_circ_0071036 expression levels into

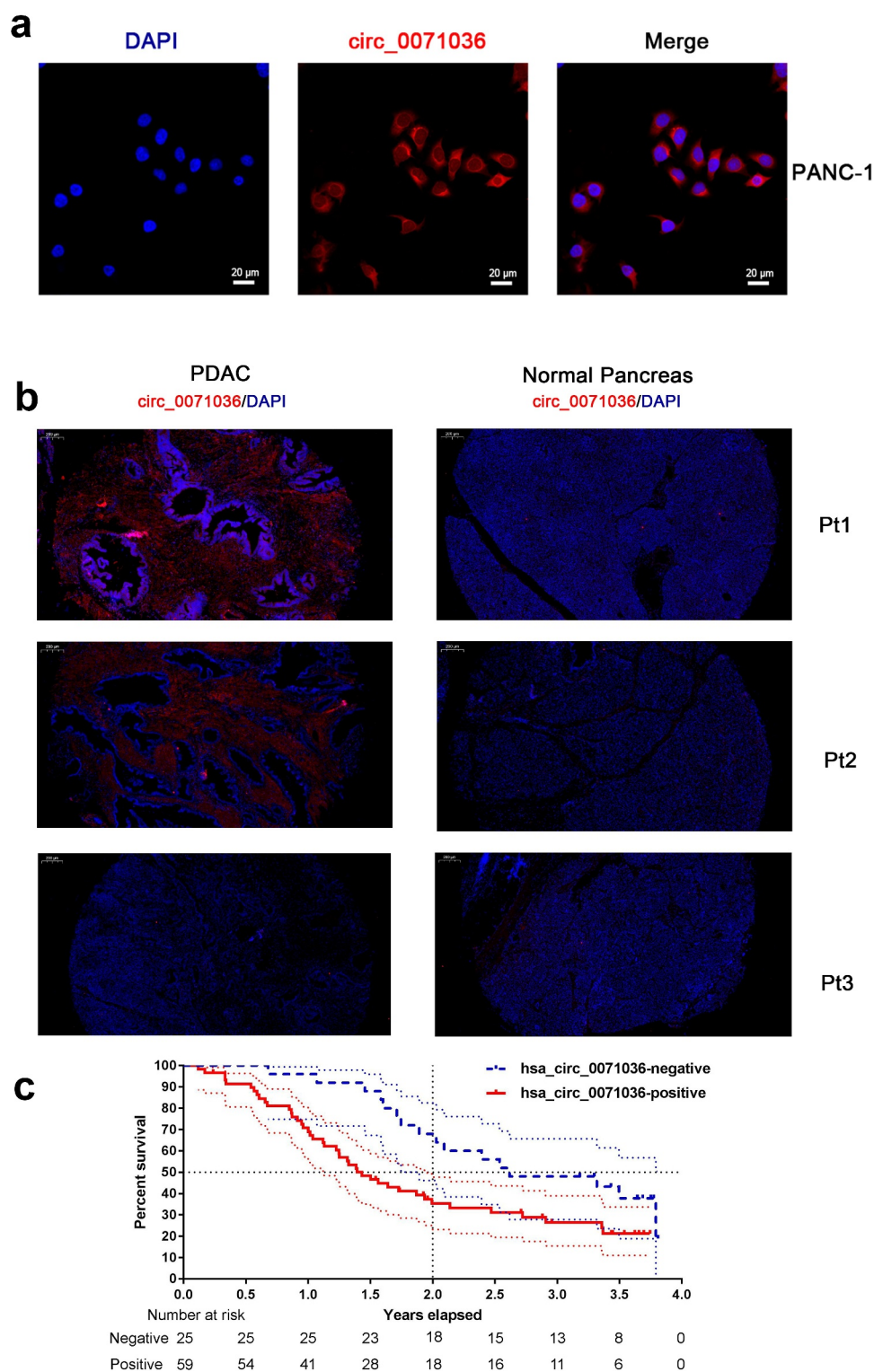


Figure 3. RNA-FISH was utilized to determine the localization of *hsa_circ_0071036* in PANC-1 cells and tissue samples. (a) Co-immunostaining of *circ_0071036* and DAPI in PANC-1 cells. (b) Co-immunostaining of *circ_0071036* and DAPI in PDAC and normal pancreas of human TMA samples (Pt1 & Pt2, positive *circ_0071036* in PDAC and negative in normal pancreas; Pt3 negative *circ_0071036* in PDAC and normal pancreas). (c) Survival analysis by differential expression of *hsa_circ_0071036* using TMA RNA-FISH.

a high expression group and a low expression group as previously mentioned in cohort 1. We demonstrat

ed that PDAC patients with regional lymph node metastases had significantly higher expression of *hsa_circ*

_0071036 ($P < 0.05$, Table 1). Interestingly, patients with higher expression of hsa_circ_0071036 were more likely to have higher PET-CT SUVmax values ($P = 0.001$, Table 1). To determine associations with patient prognosis, we then conducted survival analysis by differential expression of hsa_circ_0071036 using TMA RNA-FISH cohort 2 (Table 2). The univariate analysis showed that patients with positive hsa_circ_0071036 expression had remarkably poor prognoses than those with negative hsa_circ_0071036 expression ($P = 0.017$, Table 2, Figure 3c). Multivariate analyses also illustrated that hsa_circ_0071036 expression was an independent risk factor for OS ($P = 0.015$, Table 2).

Knockdown of hsa_circ_0071036 suppressed cell proliferation and invasion and induced apoptosis *in vitro*

To clarify the biological function of hsa_circ_0071036, we initially characterized the relationship between KRAS gene and hsa_circ_0071036 expression in human pancreatic cancer cell lines. Circ_0071036 was highly expressed in PANC-1 and AsPC-1 cells. In particular, PANC-1 and AsPC-1 cells had heterozygous and homozygous *KRAS*^{G12D} mutant status presenting relatively malignant behaviors, which were selected for subsequent experiments (Figure 4a). We next explored the role of hsa_circ_0071036 knockdown and the functional properties of PANC-1 cells *in vitro*. As shown in Figure 4b, we found that silencing hsa_circ_0071036 impaired the proliferative ability of PANC-1 cells compared with the negative control. Similarly, colony formation assays verified that knockdown of hsa_circ_0071036 had the same effect on the proliferative ability of PANC-1 cells and that si-hsa_circ_0071036 decreased the number of colonies in PANC-1 cells (Figure 4e). Furthermore, representative images and quantification results of invasion assays revealed that silencing of hsa_circ_0071036 remarkably attenuated the invasion of PANC-1 cells (Figure 4c). As illustrated in Figure 4d, flow cytometry showed that knockdown of hsa_circ_0071036 induced late apoptosis in PANC-1 cells. Together, these data indicated that hsa_circ_0071036 may function as an oncogenic circRNA in PDAC tumorigenesis.

Hsa_circ_0071036 can sponge miR-489 in PDAC

We further investigated whether hsa_circ_0071036 can function as a miRNA sponge to regulate a specific circRNA-miRNA network in PDAC cells based on two miRNA target prediction software TargetScan & miRanda, and we found that hsa_circ_0071036 might directly sponge miR-489 (Figure 5c). The miR-489 expression data were compared between pancreatic cancer tissues and corresponding adjacent normal pancreas tissues in 26 paired primary PDAC samples of cohort 1 using qRT-PCR. We verified that miR-489 was remarkably downregulated in pancreatic cancer tissue compared with the corresponding adjacent normal tissue in Figure 5a ($P < 0.001$). The decrease rate of miR-489 was 73.1% (19/26) in PDAC patients. In addition, Pearson correlation analysis demonstrated that miR-489 negatively correlated with hsa_circ_0071036 expression ($R = -0.851$, $P < 0.001$), which implies a special interaction between miR-489 and hsa_circ_0071036 in PDAC tissues. To further confirm the binding of hsa_circ_0071036 and miR-489, we conducted an RNA pull-down assay with a specific biotin-labeled hsa_circ_0071036 probe (Figure 5b). As a result, a specific enrichment of miR-489 was detected by qRT-PCR in the hsa_circ_0071036 probe group compared to the control group. As shown in Figure 5d, we next performed dual luciferase reporter activity in PANC-1 cells to validate this prediction. The results elucidated that the activity of the luciferase reporter vector expressing the wild type 3'UTR sequence of hsa_circ_0071036 could be significantly downregulated by miR-489 mimics compared with the control group ($P < 0.001$), whereas expression of miR-489 did not decrease luciferase activity driven by the mutant 3'UTR of hsa_circ_0071036 with mutated miRNA binding site. Collectively, these results suggested that hsa_circ_0071036 acts as an efficient miRNA sponge for miR-489 in PDAC (Figure 5c).

Silencing of hsa_circ_0071036 suppressed tumorigenesis of pancreatic cancer cells *in vivo*

We next evaluated the biological function of silenced hsa_circ_0071036 in the tumorigenesis of pancrea

Table 2. Survival analysis of differential expression of hsa_circ_0071036 determined using TMA RNA-FISH and clinicopathological characteristics at baseline (cohort 2).

Characteristics	N	2-year OS (%)	P value	HR (95% CI)	Multivariate analysis	
					P value	HR (95% CI)
Expression of hsa_circ_0071036						
Positive	59	35	0.017	2.0 (1.1–3.7)	0.015	3.7(1.3–10.5)
Negative	25	68	0.488	0.8 (0.5–1.4)	0.021	4.1(1.2–13.3)
Sex	54	46	<0.001	3.2 (1.8–5.7)		
Male	30	43				
Female						
Regional lymph node metastases						
Yes	40	26				
No	39	65				
Location						
Head	47	39	0.393	0.8 (0.5–1.4)		
Distal	37	52				
Neural invasion	58	44	0.235	1.5 (0.8–2.9)		
Yes	18	44				
No						
Vascular invasion						
Yes	31	59	0.001	2.5 (1.5–4.3)		
No	53	20				
Differentiation						
Grade 2	25	64	0.001	2.2 (1.4–3.3)	<0.001	4.9(2.2–10.8)
Grade 2–3	46	39				
Grade 3	10	23	0.005	1.2 (0.9–1.6)		
TNM Stage		100				
IA	1	67				
IB	3	67				
IIB	38	57				
IIA	24	20				
IIB	18	44				
III						
PET-CT SUVmax[†]						
Mean (SD)	6.2 (2.6)		<0.001	1.3 (1.1–1.4)	0.002	1.3(1.1–1.5)
Range, N	10.4, 63					
Age at onset, y[†]						
Mean (SD)	63.8 (8.7)		0.016	1.0 (0.9–1.1)		
Range, N	40, 90		<0.001	1.2 (1.0–1.5)		
Tumor size, cm[†]						
Mean (SD)	3.2 (1.4)		0.013	1.0 (0.9–1.1)		
Range, N	6.8, 90		0.024	1.0 (0.9–1.1)		
CA 19–9 level, U/mL[†]	510 (1042)					
Mean (SD)	6740, 86					
Range, N	7.0 (16.6)					
CEA level, ng/mL[†]	101.6, 77					
Mean (SD)						
Range						

[†]continuous variant

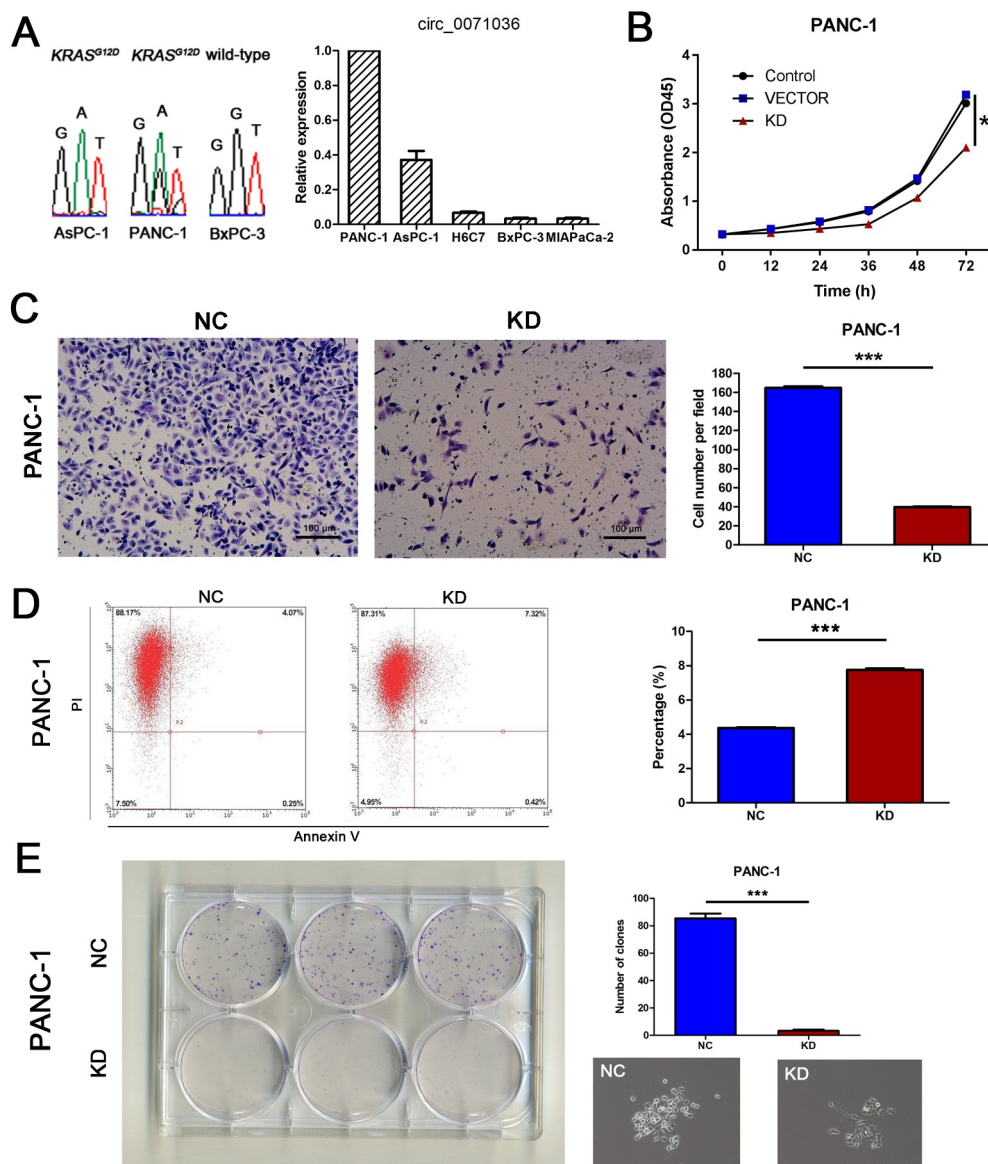


Figure 4. Effects of inhibition of *hsa_circ_0071036* on pancreatic cancer cell proliferation, colony formation, invasion and apoptosis. (a) Characterization of the *KRAS* gene and *hsa_circ_0071036* expression in the human PDAC cell lines PANC-1, AsPC-1 and BxPC-3. Left, DNA sequencing confirmed the presence of wild-type *KRAS* in BxPC-3 cells and mutant *KRAS^{G12D}* in PANC-1 and AsPC-1 cells. Right, qRT-PCR analyses of *hsa_circ_0071036* expression in various PDAC cells. (b) CCK-8 analysis revealed that inhibition of *hsa_circ_0071036* suppressed the proliferation of PANC-1 cells (one-way ANOVA). (c) Invasion assays showed that knockdown of *hsa_circ_0071036* attenuated the invasion ability of PANC-1 cells (Student's *t* test, mean \pm SEM). (d) Flow cytometry revealed that knockdown of *hsa_circ_0071036* induced late apoptosis in PANC-1 cells (Student's *t* test, mean \pm SEM). (e) Colony formation assay showed that *hsa_circ_0071036* expression had the same effect as obtained by the CCK-8 assay on PANC-1 cell growth ability (Student's *t* test, mean \pm SEM).

tic cancer cells in BALB/c nude mice (6 mice per group). Each nude mouse was injected with 5×10^6 si-Ctrl AsPC-1 cells or si-*hsa_circ_0071036* AsPC-1 cells. In comparison with the negative control group, silencing of *hsa_circ_0071036* significantly reduced

the mean tumor volume (291 ± 96 vs. 461 ± 153 , $P = 0.013$; Figure 6a,B). Regarding the tumor weight, silencing of *hsa_circ_0071036* resulted in remarkably lower tumor weight than the negative control subgroup (0.67 ± 0.18 vs. 0.92 ± 0.17 , $P = 0.033$;

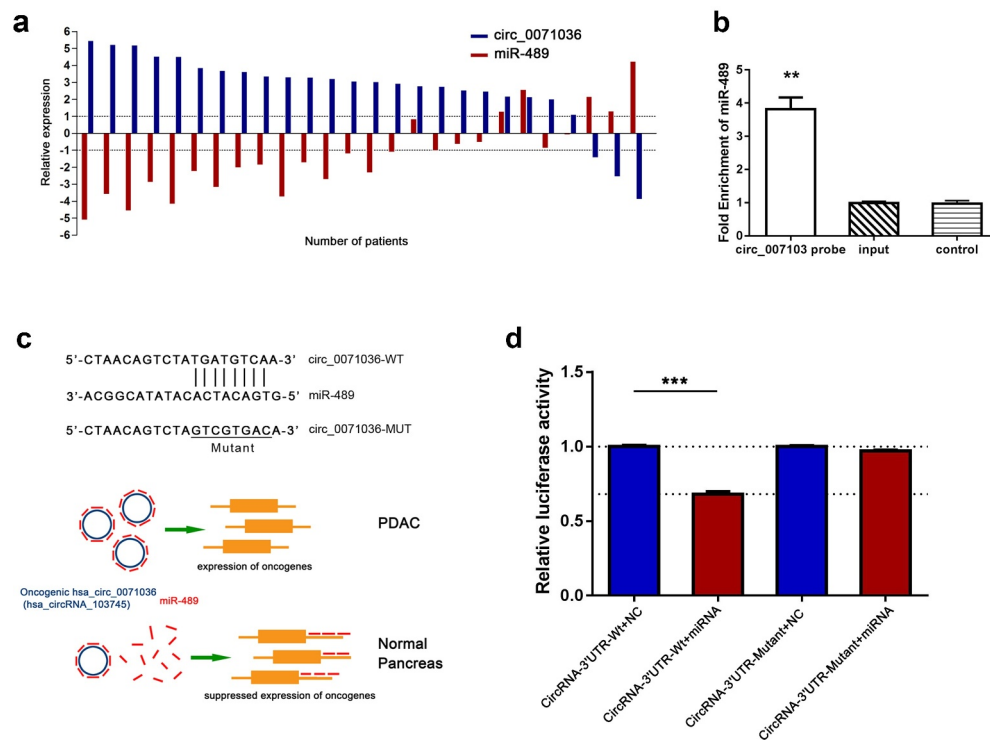


Figure 5. Hsa_circ_0071036 served as a sponge of miR-489. (a) Relative expression correlation between hsa_circ_0071036 and miR-489 in 26 paired fresh human PDAC tissues and matched adjacent normal tissues by qRT-PCR. (b) RNA pull-down assay showed that miR-489 was enriched for a specific RNA probe targeting hsa_circ_0071036, which was detected by qRT-PCR (Student's t test, mean \pm SD). (c) Top, left, the predicted wild-type and mutated miR-489 binding site in the 3'UTR of hsa_circ_0071036. A mutant miR-489 binding sequence was generated in the matched seed region. Bottom, left, schematic diagram of how hsa_circ_0071036 promotes tumorigenesis by sponging miR-489. (d) PANC-1 cells were transfected with wild-type or mutant hsa_circ_0071036 reporter plasmid, and the relative luciferase reporter activities were detected to identify the direct target site (Student's t test, mean \pm SEM).

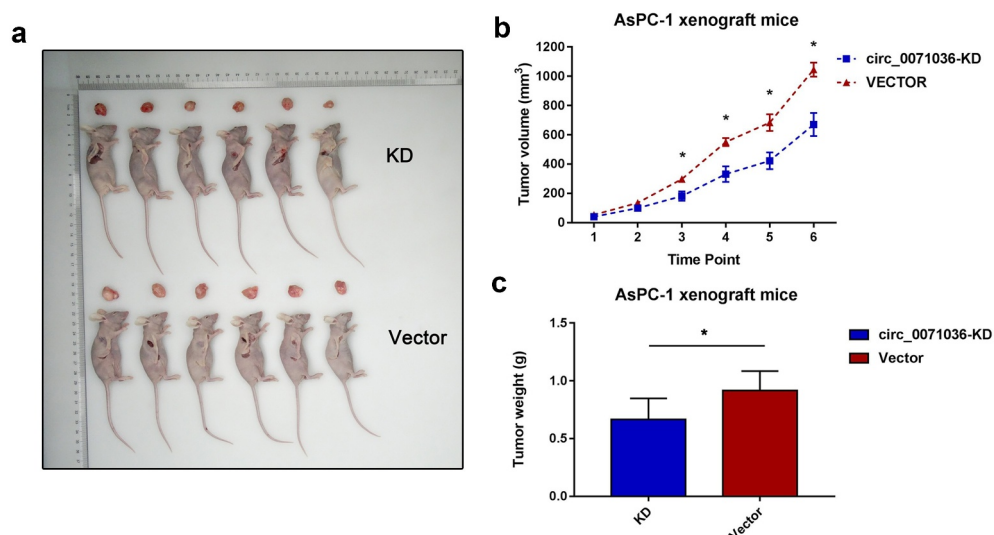


Figure 6. Inhibition of hsa_circ_0071036 suppressed the pancreatic cell growth of BALB/c xenografts. (a) Images of the xenograft tumors obtained at the endpoint from BALB/c (nu/nu) mice after injection of AsPC-1 cells transfected with si-hsa_circ_0071036 or the control vector. (b) Growth chart of tumor volume at each time point (mean \pm SEM; n = 6 mice in each group, Student's t test). (c) Weights of xenograft tumors at the endpoint (mean \pm SD, Student's t test).

Figure 6c). Thus, our findings indicated that silencing hsa_circ_0071036 may suppress tumor growth *in vivo*.

Discussion

Accumulating evidence suggests that circRNAs are dysregulated in cancers and are involved in modulating various aspects of cancer cellular properties. Remarkably, aberrant expression of circRNAs has been observed in pancreatic cancer, and the function of circRNAs in tumorigenesis, metabolism and progression is far from elucidated. Our previous studies have demonstrated that miR-489, acting downstream of KRAS/NF- κ B signaling, is a robust inhibitor of metastasis [12]. In the present study, we established that activation of hsa_circ_0071036 is a key regulator of PDAC tumorigenesis by sponging miR-489 to impair its tumor-suppressive function, which was associated with worse clinical outcomes.

By utilizing microarray analysis, our study showed that hsa_circ_0071036 (alias: hsa_circ_100395), derived from the Inositol polyphosphate 4-phosphatase type II (*INPP4B*) gene, was one of the most upregulated circRNAs in PDAC tissues. We found that hsa_circ_0071036 was significantly upregulated in PDAC tissues compared to the adjacent noncancerous tissues, and hsa_circ_0071036 contained exons and was predominantly found in the cytoplasm by morphology assays. Therefore, this evidence strongly implies that hsa_circ_0071036 is remarkably overexpressed in PDAC tissue samples and cell lines. CircRNAs are often derived from variable cleavage of pre-mRNAs, which are modulated by RNA polymerase II [13]. Recent results indicate that the expression and biological function of *INPP4B* in human cancer is controversial [14,15]. Anecdotally, a study emphasized that *INPP4B* overexpression exerts a dual function in suppressing the tumorigenicity of primary non-metastatic colorectal cancer stem-like cells while inducing the tumorigenicity of highly metastatic cells [16]. A study demonstrated *INPP4B* as a tumor suppressor in PDAC that attenuated PI3K/AKT/SGK activation [17]. Although the anti-oncogenic role

of *INPP4B* in mediating PI3K/AKT/SGK signaling in PDAC has been described, the potential interaction of hsa_circ_0071036 with its host gene *INPP4B* remains unclear.

Here, we selected pancreatic cancer cell lines with oncogenic heterozygous or homozygous *KRAS*^{G12D} mutation mimicking human PDACs for their histological features and metabolic potential to conduct *in vitro* and *in vivo* experiments. Functional experiments showed that knockdown of hsa_circ_0071036 suppressed proliferation and invasion and induced apoptosis *in vitro*. Accordingly, xenograft experiments confirmed that silencing hsa_circ_0071036 attenuated tumor growth *in vivo*. Similarly, research indicated that knockdown of oncogenic circ_0030235 inhibited cell growth and the migratory and invasive potential, and promoted cell apoptosis, while overexpression of circ_0030235 exerted the opposite effects [18]. The results by Yao and colleagues also showed that knockdown of circ-LDLRAD3 repressed the proliferation, migration and invasion of PDAC cells *in vitro* and *in vivo* [19]. Functionally, these results implied that dysregulated circRNAs may modulate pancreatic cancer KRAS-driven carcinogenesis and development.

Mounting evidence suggests that some circular RNAs contain miRNA binding sites and may function as sponges to arrest miRNA functions (ceRNA networks), abolishing the endogenous suppressive effect of miRNAs on their targeted transcripts [20,21]. Due to their small length and low abundance, most circRNAs may not serve as miRNA sponges. A study verified that circRNAs enriched in exosomes could be sorted into exosomes in producer cells and exported outside of cells to transfer biological activity to recipient cells [22]. However, recent studies including our data revealed that a number of circRNAs are relatively highly abundant in PDAC [23]. We speculated that these circRNAs could have potential biological functions in the cytoplasm. Theoretically, circRNAs cannot be displaced by the translocating ribosome due to a lack of translating capability of circRNAs, which may allow circRNAs to serve as binding platforms [24]. Coincidentally, our data also confirmed that hsa_circ_0071036 was present in the cytoplasm,

suggesting that the underlying molecular role of hsa_circ_0071036 is possible post-transcriptional regulation [25]. The bioinformatic results inferred that hsa_circ_0071036 could sequester miR-489, miR-376a, miR-376b, miR-29b and miR-608. Among them, miR-489 is a tumor suppressor that plays an important role in oncogenic KRAS-driven PDAC metastasis. Consistent with previous research results, we found that there was reciprocal repression between hsa_circ_0071036 and miR-489 expression. Mechanistically, the luciferase reporter assay indicated that hsa_circ_0071036 acts as an efficient miRNA sponge for miR-489. More importantly, RNA pull-down analysis illustrated that miR-489 was enriched for a specific RNA probe targeting hsa_circ_0071036. Taken together, these lines of evidence reveal that the hsa_circ_0071036/miR-489 axis might participate in tumourigenesis and progression of PDAC.

Clinically, we reported that hsa_circ_0071036, as a diagnostic biomarker, was predominantly positive in PDAC patients and could provide a good compromise between specificity and sensitivity. More importantly, we confirmed that dysregulated hsa_circ_0071036 correlated with unfavorable clinicopathological characteristics and poor prognosis of PDAC patients. Therefore, patients with upregulated hsa_circ_0071036 were more likely to have higher PET-CT SUV_{max} values. In hypovascularized and stroma-rich pancreatic cancer, glutamine and glucose metabolism is reprogrammed by oncogenic KRAS to support rapid cell proliferation and to allow cells to efficiently adapt and survive to a nutrient-restricted microenvironment [26]. We speculated that the hsa_circ_0071036/miR-489 axis may participate in this process because of significant related glucose uptake, which is resistant to metabolic stress, including hypoxia and nutrient deprivation. In addition, dysregulated miR-489 could not suppress ADAM9 and MMP7, which function to remodel the extracellular matrix, thereby facilitating the metastasis of cancer cells [12]. This was consistent with our finding that upregulated hsa_circ_0071036 were more prone to regional lymph node metastases. These results ensured that aberrant expression of hsa_circ_0071036 could be applied to facilitate diagnosis and predict prognosis in PDAC to help make therapeutic decisions.

In conclusion, this study revealed that dysregulated hsa_circ_0071036 promotes PDAC pathogenesis and progression by directly sponging miR-489, which implies an important role for the interaction network of hsa_circ_0071036 and miR-489 in pancreatic cancer. Further study with a large cohort of PDAC patients is necessary to validate its clinical implications.

Acknowledgments

This study was supported by the National Natural Science Foundation of China (81702304, 81773068) and the Shanghai Shen Kang Hospital Development Center (SHDC12017X04).

Disclosure statement

All authors declare that they have no conflict of interest.

Funding

This work was supported by the National Natural Science Foundation of China [81702304]; National Natural Science Foundation of China [81773068]; Shanghai Shen Kang Hospital Development Center [SHDC12017X04].

ORCID

Xu Han  <http://orcid.org/0000-0002-0238-543X>

Yaolin Xu  <http://orcid.org/0000-0002-0971-518X>

References

- [1] Siegel RL, Miller KD, Jemal A. Cancer statistics, 2018. *CA Cancer J Clin.* 2018;68:7–30.
- [2] Waddell N, Pajic M, Patch AM, et al. Whole genomes redefine the mutational landscape of pancreatic cancer. *Nature.* 2015;518:495–501.
- [3] Hessmann E, Johnsen SA, Siveke JT, et al. Epigenetic treatment of pancreatic cancer: is there a therapeutic perspective on the horizon? *Gut.* 2017;66:168–179.
- [4] Herbst B, Zheng L. Precision medicine in pancreatic cancer: treating every patient as an exception. *Lancet Gastroenterol Hepatol.* 2019;4:805–810.
- [5] Memczak S, Jens M, Elefsinioti A, et al. Circular RNAs are a large class of animal RNAs with regulatory potency. *Nature.* 2013;495:333–338.
- [6] Szabo L, Salzman J. Detecting circular RNAs: bioinformatic and experimental challenges. *Nat Rev Genet.* 2016;17:679–692.

- [7] Kristensen LS, Andersen MS, Stagsted LVW, et al. The biogenesis, biology and characterization of circular RNAs. *Nature reviews Genetics*. 2019;20:675–691.
- [8] Weng W, Wei Q, Toden S, et al. Circular RNA ciRS-7-A promising prognostic biomarker and a potential therapeutic target in colorectal cancer. *Clin Cancer Res*. 2017;23:3918–3928.
- [9] Chen X, Chen RX, Wei WS, et al. PRMT5 circular RNA promotes metastasis of urothelial carcinoma of the bladder through sponging miR-30c to induce epithelial-mesenchymal transition. *Clin Cancer Res*. 2018;24:6319–6330.
- [10] Meng J, Chen S, Han JX, et al. Twist1 regulates vimentin through Cul2 circular RNA to promote EMT in hepatocellular carcinoma. *Cancer Res*. 2018;78:4150–4162.
- [11] Li J, Li Z, Jiang P, et al. Circular RNA IARS (circ-IARS) secreted by pancreatic cancer cells and located within exosomes regulates endothelial monolayer permeability to promote tumor metastasis. *J Exp Clin Cancer Res*. 2018;37:177.
- [12] Yuan P, He XH, Rong YF, et al. KRAS/NF-kappaB/YY1/miR-489 signaling axis controls pancreatic cancer metastasis. *Cancer Res*. 2017;77:100–111.
- [13] Li X, Yang L, Chen LL. The biogenesis, functions, and challenges of circular RNAs. *Mol Cell*. 2018;71:428–442.
- [14] Chen Y, Sun Z, Qi M, et al. INPP4B restrains cell proliferation and metastasis via regulation of the PI3K/AKT/SGK pathway. *J Cell Mol Med*. 2018;22:2935–2943.
- [15] Gasser JA, Inuzuka H, Lau AW, et al. SGK3 mediates INPP4B-dependent PI3K signaling in breast cancer. *Mol Cell*. 2014;56:595–607.
- [16] Yang L, Ding C, Tang W, et al. INPP4B exerts a dual function in the stemness of colorectal cancer stem-like cells through regulating Sox2 and Nanog expression. *Carcinogenesis*. 2019. DOI:10.1093/carcin/bgz110
- [17] Zhang B, Wang W, Li C, et al. Inositol polyphosphate-4-phosphatase type II plays critical roles in the modulation of cadherin-mediated adhesion dynamics of pancreatic ductal adenocarcinomas. *Cell Adh Migr*. 2018;12:548–563.
- [18] Xu Y, Yao Y, Gao P, et al. Upregulated circular RNA circ_0030235 predicts unfavorable prognosis in pancreatic ductal adenocarcinoma and facilitates cell progression by sponging miR-1253 and miR-1294. *Biochem Biophys Res Commun*. 2019;509:138–142.
- [19] Yao J, Zhang C, Chen Y, et al. Downregulation of circular RNA circ-LDLRAD3 suppresses pancreatic cancer progression through miR-137-3p/PTN axis. *Life Sci*. 2019;239:116871.
- [20] Zheng Q, Bao C, Guo W, et al. Circular RNA profiling reveals an abundant circHIPK3 that regulates cell growth by sponging multiple miRNAs. *Nat Commun*. 2016;7:11215.
- [21] Bonizzato A, Gaffo E, Te Kronnie G, et al. CircRNAs in hematopoiesis and hematological malignancies. *Blood Cancer J*. 2016;6:e483.
- [22] Li Y, Zheng Q, Bao C, et al. Circular RNA is enriched and stable in exosomes: a promising biomarker for cancer diagnosis. *Cell Res*. 2015;25:981–984.
- [23] Li H, Hao X, Wang H, et al. Circular RNA expression profile of pancreatic ductal adenocarcinoma revealed by microarray. *Cell Physiol Biochem*. 2016;40:1334–1344.
- [24] Guo JU, Agarwal V, Guo H, et al. Expanded identification and characterization of mammalian circular RNAs. *Genome Biol*. 2014;15:409.
- [25] Salzman J. Circular RNA expression: its potential regulation and function. *Trends Genet*. 2016;32:309–316.
- [26] Son J, Lyssiotis CA, Ying H, et al. Glutamine supports pancreatic cancer growth through a KRAS-regulated metabolic pathway. *Nature*. 2013;496:101–105.